

---

This is an electronic reprint of the original article.  
This reprint may differ from the original in pagination and typographic detail.

Tripathi, Tripurari Sharan; Wilken, Martin; Hoppe, Christian; de los Arcos, Teresa;  
Grundmeier, Guido; Devi, Anjana; Karppinen, Maarit  
**Atomic Layer Deposition of Copper Metal Films from  $\text{Cu}(\text{acac})_2$  and Hydroquinone Reductant**

*Published in:*  
Advanced Engineering Materials

*DOI:*  
[10.1002/adem.202100446](https://doi.org/10.1002/adem.202100446)

Published: 01/10/2021

*Document Version*  
Publisher's PDF, also known as Version of record

*Published under the following license:*  
CC BY-NC-ND

*Please cite the original version:*  
Tripathi, T. S., Wilken, M., Hoppe, C., de los Arcos, T., Grundmeier, G., Devi, A., & Karppinen, M. (2021). Atomic Layer Deposition of Copper Metal Films from  $\text{Cu}(\text{acac})_2$  and Hydroquinone Reductant. *Advanced Engineering Materials*, 23(10), Article 2100446. <https://doi.org/10.1002/adem.202100446>

---

This material is protected by copyright and other intellectual property rights, and duplication or sale of all or part of any of the repository collections is not permitted, except that material may be duplicated by you for your research use or educational purposes in electronic or print form. You must obtain permission for any other use. Electronic or print copies may not be offered, whether for sale or otherwise to anyone who is not an authorised user.

# Atomic Layer Deposition of Copper Metal Films from $\text{Cu}(\text{acac})_2$ and Hydroquinone Reductant

Tripurari Sharan Tripathi, Martin Wilken, Christian Hoppe, Teresa de los Arcos, Guido Grundmeier, Anjana Devi, and Maarit Karppinen\*

High-quality copper metal thin films are demanded for a number of advanced technologies. Herein, a facile ALD (atomic layer deposition) process for the fabrication of Cu metal films directly from two solid readily usable precursors, copper acetylacetonate as the source of copper and hydroquinone as the reductant is reported. This process yields highly crystalline, dense, specularly reflecting, and electrically conductive Cu films with an appreciably high growth rate of 1.8 Å/cycle at deposition temperatures as low as 160 to 240 °C.

processes for high-quality Cu metal films to meet all the specific requirements of the targeted applications. Ultimately, the ALD Cu films should be made competitive with the current commercial technology based on PVD (physical vapor deposition) and plating techniques; this would require low enough resistivity values and the avoidance of any agglomeration problems leading to rough and even discontinuous films at small film thicknesses.

There are several direct or indirect ALD processes for copper metal thin films, as shown in **Table 1**, and discussed in more detail e.g., in a recent review by Hagen et al.<sup>[4]</sup> on metal thin film fabrications by ALD. For copper itself, the repertoire of well-behaving precursors is already significantly wide. Most of the processes use  $\text{H}_2$  as the reductant, but the difficulty is its limited reactivity which implies unsatisfactorily low growth rates particularly at low deposition temperatures. Hydrogen plasma is more reactive, but the film conformality is often the issue. In few works, organic reactants have been investigated as well.<sup>[5–7]</sup> Organics are typically in solid or liquid form, and hence relatively easy to handle. Recently, we developed a new promising ALD Cu process based on  $\text{Cu}(\text{acac})_2$  (acac: acetylacetonate) as the source of copper and a mixture of hydroquinone (HQ) and water to serve as the reductant.<sup>[8]</sup> The process offered appreciably high growth rates up to 1.9 Å/cycle; yet, the purity of the films, judged only indirectly from the electrical transport measurements, remained to be improved. Another weakness in our  $\text{Cu}(\text{acac})_2 + \text{HQ}/\text{H}_2\text{O}$  process was its complexity due to the involvement of three precursors.

Here, in the present study we have hypothesized that HQ is the primary reductant, and it could be possible to optimize the process to work without the intermittent water pulses for hydroxylation. We will demonstrate that this indeed is the case, and high-quality Cu films can be directly deposited from only the two precursors,  $\text{Cu}(\text{acac})_2$  and HQ, in a wide deposition temperature range starting from as low temperature as 160 °C. X-ray photoelectron spectroscopy (XPS) measurements confirm the metallic state for copper, with the carbon level below 9 at.% (i.e., HQ/Cu ratio less than 1.5%).

## 1. Introduction

Copper metal is of high preference in microelectronics for interconnections due to its low resistivity and high resistance to electromigration.<sup>[1]</sup> The fact that the dimensions of the smallest features in microelectronic devices are scheduled to reach the 3-nm limit by 2022,<sup>[2]</sup> has set increasingly strict demands for the technique to deposit continuous low-resistivity Cu films for the device fabrication. Atomic layer deposition (ALD) —a leading gas-phase thin-film technique based on alternately pulsed precursors —is an ideal choice for microelectronics industry, as it inherently provides highly conformal thin films over complex geometries and high-aspect-ratio structures, and allows sub-nanometer control over the film thickness.<sup>[3]</sup> The challenge is to find industry-feasible, efficient and reliable ALD

T. S. Tripathi, M. Karppinen  
Department of Chemistry and Materials Science  
Aalto University  
FI-00076 Aalto, Finland  
E-mail: maarit.karppinen@aalto.fi

M. Wilken, A. Devi  
Department of Chemistry  
Ruhr University Bochum  
Universitätsstr., 44801 Bochum, Germany

C. Hoppe, T. de los Arcos, G. Grundmeier  
Paderborn University  
Germany

 The ORCID identification number(s) for the author(s) of this article can be found under <https://doi.org/10.1002/adem.202100446>.

© 2021 The Authors. Advanced Engineering Materials published by Wiley-VCH GmbH. This is an open access article under the terms of the Creative Commons Attribution-NonCommercial-NoDerivs License, which permits use and distribution in any medium, provided the original work is properly cited, the use is non-commercial and no modifications or adaptations are made.

DOI: 10.1002/adem.202100446

## 2. Results and Discussion

All our deposition tests for the  $\text{Cu}(\text{acac})_2 + \text{HQ}$  process yielded crystalline Cu metal films which were visually uniform, shiny, and specularly reflecting. We first systematically investigated the effects of the different deposition parameters on the film

**Table 1.** ALD processes for Cu metal thin films.

Metal precursor/Reductant	Deposition temp. (°C)*	GPC (Å/cycle)	Ref.
Cu(thd) <sub>2</sub> /H <sub>2</sub>	190–260	0.3	[14]
	350	2.1	[31]
Cu(acac) <sub>2</sub> /H <sub>2</sub>	250	–	[32]
[Cu-( <sup>t</sup> BuNCMeN <sup>t</sup> Bu)] <sub>2</sub> /H <sub>2</sub>	150–250	0.04	[33–35]
[( <sup>t</sup> Bu <sub>3</sub> P) <sub>2</sub> Cu(acac)]/wet O <sub>2</sub>	100–125	0.1	[36]
Cu(hfac) <sub>2</sub> /isopropanol	260	–	[20]
Cu(amd)/H <sub>2</sub> plasma	50–100	0.7	[37]
[Cu( <sup>i</sup> PrNHC)(hmds)]/Ar/H <sub>2</sub> plasma	200	0.2	[38]
[Cu( <sup>t</sup> BuNHC)(hmds)]/Ar/H <sub>2</sub> plasma	100	0.23	[39]
Cu( <sup>t</sup> Bu-amd) <sub>2</sub> +NH <sub>3</sub> /H <sub>2</sub>	160	0.15	[34]
Cu(dmap) <sub>2</sub> /ZnEt <sub>2</sub>	100–120	0.2	[40,41]
CuCl/H <sub>2</sub>	360, 400	0.8	[42,43]
Cu(OCHMeCH <sub>2</sub> NMe <sub>2</sub> ) <sub>2</sub> +formic acid/hydrazine	100–170	0.5	[7]
Cu(OCHMeCH <sub>2</sub> NMe <sub>2</sub> ) <sub>2</sub> /H <sub>2</sub> plasma	100–180	0.65	[44]

\*So-called ALD window, or if this is not reported, the lowest deposition temperature used.

growth characteristics. **Figure 1(a)** shows the dependence of the film thickness (for the number of ALD cycles fixed to 600) on the deposition temperature in the temperature range, 160–240 °C; for these experiments the precursor/purge pulse times were fixed as follows: 2 s Cu(acac)<sub>2</sub>/3 s N<sub>2</sub>/2 s HQ/3 s N<sub>2</sub>. It can be seen that the film thickness first decreases sharply between 160–180 °C, retains essentially constant between 180–220 °C, and then slightly decreases again above 220 °C. We also calculated the mass density of films from the XRR data, and noticed that within 180–200 °C it remained essentially constant whereas being lower both below 180 °C and above 200 °C. Thus, we concluded that the growth is optimal in the temperature range, 180–200 °C. For the rest of the process optimization experiments, we fixed the deposition temperature to 190 °C.

To ascertain the saturation of the surface reactions during the ALD cycles, we then investigated the effects of the precursor

pulse lengths on the film growth rate, see **Figure 1(b)** where we have gradually increased the pulse/purge durations for one of the precursors at a time (whereas keeping the durations fixed at 2 s/3 s for the other); the number of deposition cycles was fixed to 200 for these experiments. It can be seen that the growth-per-cycle (GPC) value essentially saturates for both precursors when the precursor pulse length is 2 s or longer, to yield the Cu films with the growth rate of ≈ 1.8 Å/cycle. Finally, in **Figure 1(c)** shows that with these deposition parameters (190 °C; precursor/purge pulse lengths 2 s/3 s) the film thickness is perfectly controlled by the number of ALD cycles applied. The slope of the linear fit line gives us the GPC value at 1.75 Å/cycles. Comparing this growth rate value to the values shown in **Table 1** for the other reported ALD processes of metallic Cu films reveals that our Cu(acac)<sub>2</sub> + HQ process is several magnitudes more efficient than these other processes at low temperatures (below 200 °C). It should also be mentioned that the growth rate characteristics achieved here for the water-free process are not inferior to our original Cu(acac)<sub>2</sub> + HQ/H<sub>2</sub>O process.<sup>[8]</sup> For the further sample characterizations, we grew the films with 600 ALD cycles, to achieve ≈ 100 nm thick films.

**Figure 2**, shows the GIXRD patterns for the films deposited at different temperatures from 160 to 240 °C. It is clear that our Cu(acac)<sub>2</sub> + HQ process yields highly crystalline Cu metal films throughout the deposition temperature range investigated with no (crystalline) foreign inclusions or traces of copper oxide phases as an impurity. The left inset in the figure displays the normalised XRR plots at an expanded scale. Critical angle in XRR measurements gives a rough estimate of the surface electron density of the films and thus an estimate of the mass density of films, assuming a homogenous, smooth, and continuous deposition. The higher the surface electron density of a material is, the higher is the critical angle for the film.<sup>[9]</sup> The right inset shows the mass density values as a function of deposition temperature calculated from the critical angles of the films. It can be seen that within 180–200 °C the density remains essentially constant at ≈ 8.0 g cm<sup>-3</sup> (which is close to the ideal density of metallic copper, 8.9 g cm<sup>-3</sup>), while being lower both below 180 °C and above 200 °C. The slightly lower density at low temperatures is in line with the observed agglomerate type of growth in SEM images at low temperatures. Then, the sharp decrease in density

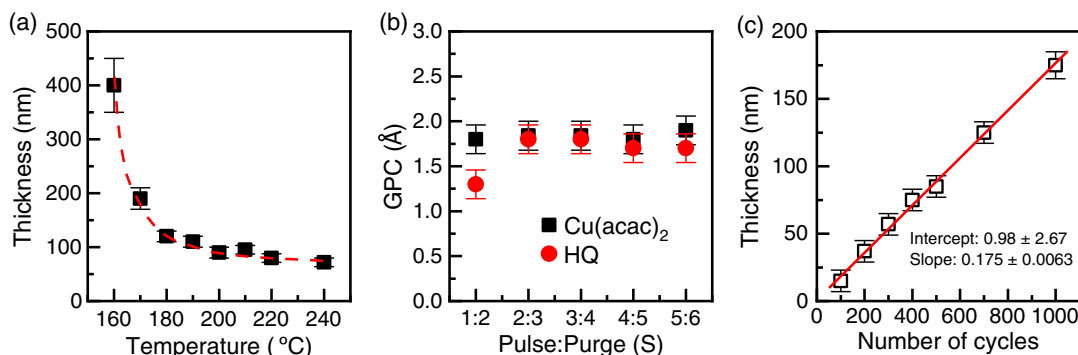


**Figure 1.** Investigation of deposition parameters for the Cu(acac)<sub>2</sub> + HQ process. a) Film thickness as a function of deposition temperature; the red dotted line is a guide for the eyes b) Film growth-per-cycle (GPC) at 190 °C as a function of the pulse:purge durations (x sec. pulse : y sec. purge) for the two precursors, Cu(acac)<sub>2</sub> and HQ. c) Film thickness as a function of the number of deposition cycles at 190 °C; the red solid line is a linear fit to the data. In a) and c), the pulse/purge times were 2 s Cu(acac)<sub>2</sub>/3 s N<sub>2</sub>/2 s HQ/3 s N<sub>2</sub>.

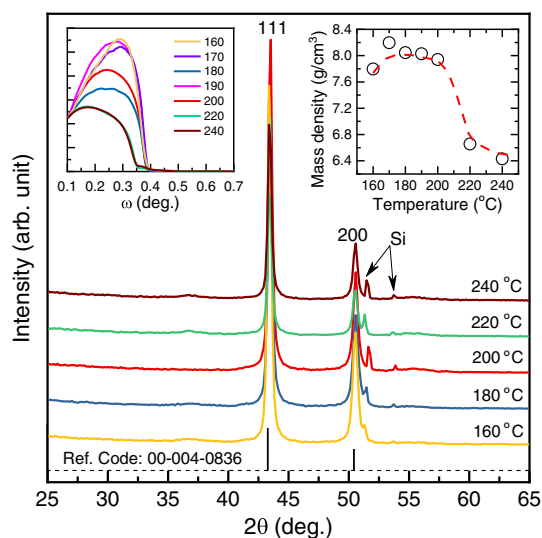


**Figure 2.** GIXRD patterns for the films deposited at several temperatures. Left inset shows the XRR data at an expanded scale around the critical angle (normalised at start angle for minimum counts), and the right inset shows the mass density as a function of deposition temperature, calculated from the critical angle estimated from the XRR plot by taking derivatives of the data; the red dotted curve is a guide to the eyes.

above 220 °C may be due to partial decomposition of the copper precursor; there are reports indicating that  $\text{Cu}(\text{acac})_2$  starts to decompose above 210 °C.<sup>[10]</sup>

To assess the surface morphology and topological features of the films in more detail, as shown in **Figure 3** both AFM and SEM images for representative films. For each film, there is a good correspondence between the AFM and SEM images. From SEM images dense and continuous films are readily visible. Films deposited at lower temperatures have larger grains and show micro-agglomerate-like features along with the highest RMS roughness values (up to 35 nm). As the deposition temperature increases, the grain size decreases and the homogeneity improves, and accordingly the RMS roughness value decreases to 8 nm for the film deposited at 200 °C.

To confirm the metallic state of copper and address the possible impurities in our Cu metal thin films, XPS measurements were performed on films deposited at 200 °C. The survey spectrum of the sample measured as-introduced shows mainly contributions from Cu (~13 at.%), O (~27 at.%) and C (~58 at.%) and trace amounts of N (<1 at.%) and Cl (<1 at.%). After sputtering the sample during 3 min with Ar ions at 3 keV, the composition of the sample is mainly Cu (86 at.%), with smaller contributions from O (5 at.%) and C (9 at.%), possibly due to traces of HQ (1%-2%) left in the sample. No traces of N or Cl were seen after sputtering. The core levels of  $\text{Cu}2p_{3/2}$ , O1s and C1s for the sample before and after sputtering are shown in **Figure 4**. The  $\text{Cu}2p_{3/2}$  peak of the sample as introduced (a.i.) shows two components at 932.6 and 934.7 eV corresponding respectively to metallic Cu and  $\text{CuO}$ .<sup>[11]</sup> The oxide component is due to superficial oxidation from contact with ambient air, and it disappears after the sputtering, confirming the successful deposition of metallic Cu, in agreement with the GIXRD results.

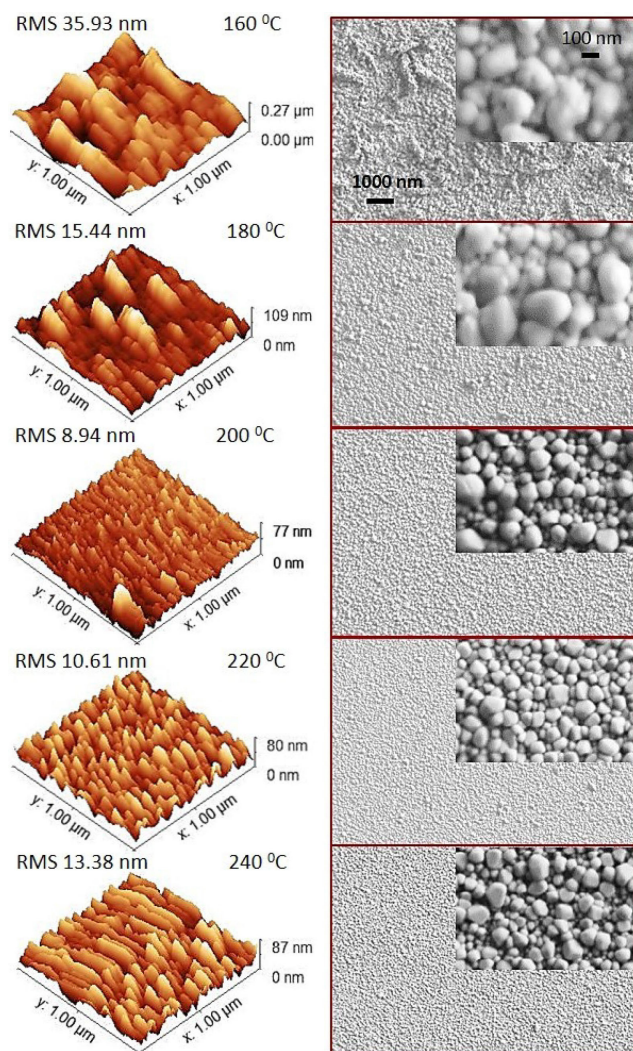


**Figure 3.** AFM (left) and SEM (right) images for the films deposited at temperatures 160–240 °C.

The interpretation of the O1s and C1s peaks is not straightforward, due to the possible coexistence of remains of the original HQ, its oxidized byproduct p-benzoquinone (BQ), and unidentified adventitious carbon species. The C1s peak in the a.i. measurement shows three components at 284.7 eV (C–C or C–H bonds), 286.1 eV (C–O) and 288.5 eV (C = O) that can be associated to adventitious carbon. The corresponding O1s peak shows three components, which can be roughly associated to Cu–O bonds (530.4 eV), C = O bonds (531.8 eV) and C–O bonds (533.3 eV).<sup>[12]</sup> It is unclear from the spectrum whether any of these components could be masking the presence of HQ (C1s at 283.5 and 285.1 eV; O1s at 532.2 eV) or BQ (with C1s at 283.4 and 286.0 eV; O1s at 530.8 eV).<sup>[13]</sup> After sputtering, the remaining C1s peak can be decomposed into one relatively broad component at 284.2 eV and two weak components at 285.6 and 287.7 eV. The corresponding O1s peak shows two components at 530.1 and 531.7 eV. The shapes of the C1s and O1s peaks do not allow for a univocal assignment to HQ or BQ within the film. However, they are compatible with the interpretation that they

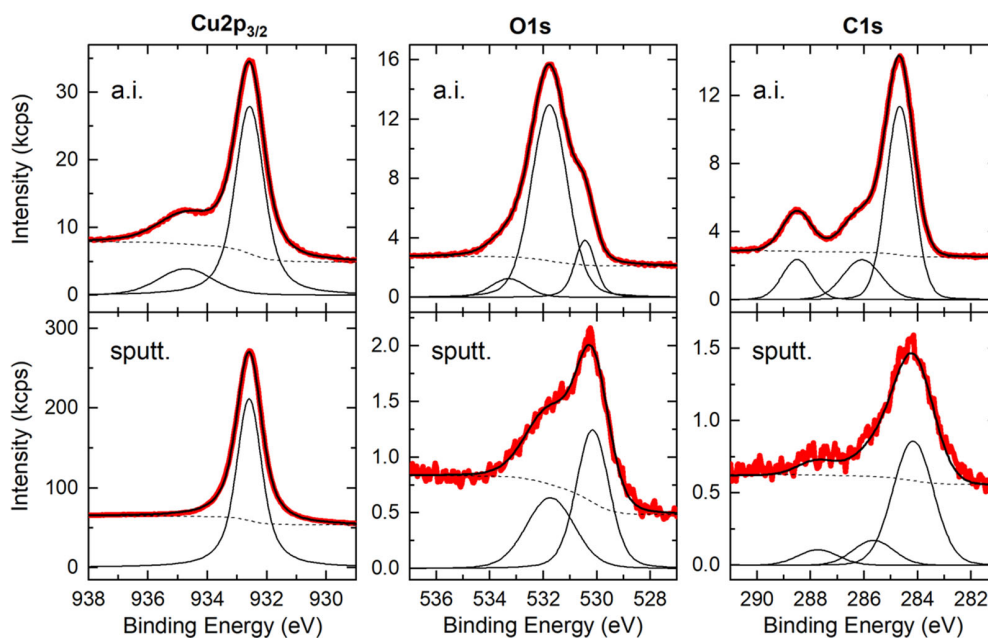


**Figure 4.** XPS spectra corresponding to  $\text{Cu}2p_{3/2}$ ,  $\text{O}1s$  and  $\text{C}1s$  core levels of a thin film sample grown at  $200^\circ\text{C}$ . Upper row: sample measured as introduced (a.i.). Lower row: sample measured after 3 min sputtering at 3 keV within the XPS spectrometer chamber (sputt.). Thick red lines: original spectra; thick black lines: sum spectra; thin black lines: line components; discontinuous black lines: background.

correspond to original HQ of BQ compounds existing within the film, which could have been partially broken during the sputter treatment.

as shown in **Figure 5** the dependence of electrical resistivity ( $\rho$ ) on temperature for the films deposited at 160, 180, and  $200^\circ\text{C}$ , after subtracting the temperature independent residual resistivity component. The somewhat high residual resistivity contribution ( $\approx 30\ \mu\Omega\text{-cm}$ ) correlates well with the higher surface carbon impurity contribution in the XPS measurements for the as-deposited (non-sputtered) films. A perfect metallic conduction behavior ( $d\rho/dT > 0$ ) is seen for all the three films. Also seen is that the resistivity values slightly decrease with increasing deposition temperature, presumably reflecting the surface

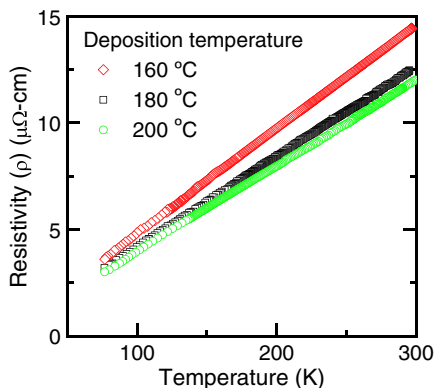


**Figure 5.** Electrical resistivity ( $\rho$ ) as a function of temperature for films deposited at different temperatures, after subtracting the temperature independent residual resistivity component. Residual resistivity was calculated by extrapolating the linear curves to zero Kelvin.

quality of the films, as surface roughness and scattering from grain boundaries naturally increase the film resistivity. The room temperature resistivity values are in the range of  $10\text{--}15\ \mu\Omega\text{-cm}$ , i.e., very similar or lower than those previously reported for ALD-grown Cu metal films with comparative thicknesses (ranging from  $\approx 6.4$  to  $89\ \mu\Omega\text{-cm}$ ),<sup>[5,7,14]</sup> but somewhat higher than the ultimate target value of  $1.72\ \mu\Omega\text{-cm}$  at  $20^\circ\text{C}$  for the bulk resistivity of copper.

Finally, we like to mention that there are a few previous reports of the ALD of copper metal films using organic reductants. For example, Waechtler et al.<sup>[15]</sup> used formic acid (assisted by a Ru catalyst) as the reductant to reduce  $\text{Cu}_2\text{O}$  grown from  $(^t\text{Bu}_3\text{P})_2\text{Cu}(\text{acac})$  ( $\text{Bu} = \text{butyl}$ ) and wet  $\text{O}_2$  to metallic Cu, whereas Knisley et al.<sup>[7]</sup> used hydrazine to reduce copper formate. In a few other non-ALD gas-phase processes, aliphatic alcohols have been used as a reductant. For example, in chemical fluid deposition (CFD)<sup>[16]</sup> and chemical vapour deposition (CVD),<sup>[17–19]</sup> methanol, ethanol, and isopropanol have been used to produce Ni, Co, and Cu metal films from metal acetylacetonate precursors. In CVD,  $\text{Cu}(\text{acac})_2$  is first reacted with  $\text{H}_2\text{O}$  to yield  $\text{Cu}_2\text{O}$  through ligand-exchange reaction,<sup>[20–23]</sup> which is then reduced to Cu metal in a separate reduction step. In the present ALD process,  $\text{Cu}(\text{acac})_2$  is directly reduced by hydroquinone. It is known that HQ can be oxidized in the presence of both Cu(I) and C(II) species.<sup>[24]</sup> Also, the ability of copper metal to catalyze the oxidation of HQ to benzoquinone (BQ) has been verified in several other studies.<sup>[25–27]</sup> Thus, in our  $\text{Cu}(\text{acac})_2 + \text{HQ}$  process, HQ should have the capacity to reduce Cu(II) from  $\text{Cu}(\text{acac})_2$ , liberating BQ as the reduction product. The forming Cu metal surface should be beneficial to promote this reaction. To provide experimental evidence for the feasibility of this reaction mechanism, we conducted a solid state reactions with the two reactants,

Cu(acac)<sub>2</sub> and HQ, using Schlenk flasks and recorded the NMR and IR data on the liberated byproduct which was confirmed to be BQ (Figures S2, S3, Supporting Information). The forming Cu metal surface that was deposited on the Schlenk flask was a proof for the reduction of the Cu(II) precursor by HQ (Figure S1, Supporting Information) and this should be beneficial to promote this reaction. To achieve the continuation of the surface reactions between the alternately pulsed Cu(acac)<sub>2</sub> and HQ precursors in ALD, it is then important that the incoming Cu(acac)<sub>2</sub> molecules can adsorb on the formed Cu metal surface. Indeed, Hu et al.<sup>[28]</sup> have demonstrated the adsorption of Cu(acac)<sub>2</sub> onto Cu(110) surfaces. Thus, the binary ALD process, Cu(acac)<sub>2</sub> + HQ, can continue without additional reactants. Further experimental evidence from e.g., thermal desorption mass spectrometry of the elements at the exhaust stages would be valuable for the validation of this reaction scheme.

### 3. Conclusion

We have developed a new promising ALD process for in-situ deposition of copper metal thin films at low temperatures. The process is based upon sequentially pulsed Cu(acac)<sub>2</sub> and hydroquinone (HQ) precursors, and it yields highly crystalline copper metal films with an appreciably high growth rate of  $\approx 1.8 \text{ \AA/cycle}$  at low deposition temperatures even below 200 °C. The carbon level is 9 at. % or less according to XPS, implying the traces of HQ being below 1–2 at.%. The films are highly crystalline and dense, and visually shiny and specularly reflecting; they show perfect metallic-type behavior in resistivity versus temperature measurements, with room-temperature resistivity values as low as 10–15  $\mu\Omega\cdot\text{cm}$ . These values are competitive for ALD-grown Cu metal films, but yet higher than desired for real applications. In future works, true process development efforts preferably in clean-room environment should be made to approach the ultimate targets for the film quality.

As for the underlining chemistry, we propose the oxidation of the organic HQ (hydroquinone) precursor as the possible mechanism responsible for the in-situ growth of metallic copper, followed by adsorption of the Cu(acac)<sub>2</sub> precursor on the Cu surface in the next step to realize the continuation of the layer-by-layer film growth. To prove this concept, theoretical studies using density functional theory (DFT) and further in-situ mechanistic studies are needed to truly consolidate this conjecture.

### 4. Experimental Section

The deposition process is based on an ALD cycle of two precursors only, i.e., Cu(acac)<sub>2</sub> and HQ, pulsed into the reactor in a sequence, using high purity nitrogen (99.999%) as the carrier and purge gas at 300 sccm. The precursors were procured from commercial sources (Cu(acac)<sub>2</sub> from STREM chemicals, purity 97%; HQ from Alfa Aesar, purity 98%). For the depositions these precursors were placed inside the reactor and heated at 130 and 95 °C, respectively, for sublimation. The depositions were conducted in a commercial hot-wall flow-type ALD reactor (F-120, ASM Microchemistry Ltd., Finland), operated under a nitrogen gas pressure of 2–3 mbar. The films were deposited on 3.5 × 3.5 cm<sup>2</sup> borosilicate glass and silicon (without removing the native oxide layer) substrates.

Grazing-incidence X-ray diffraction (GIXRD: grazing incidence angle of 1°) and X-ray reflectivity (XRR) measurements (PAN analytical model X'pert Pro; CuK<sub>α</sub>) were performed to assess the crystallinity/phase

composition and density of the films, respectively. The as-deposited films were crystalline and did not show the typical fringe patterns in XRR measurement. Thus, to determine the thickness of the films, cantilever tip jump technique of atomic force microscope (AFM; TopoMetrix Explorer); details of these analyses were as in our previous work.<sup>[29]</sup> The same AFM was also used for the surface topography and root-mean-square (RMS) roughness measurements. Scanning electron microscopy (SEM; Zeiss–Sigma VP, resolution 1.3 nm @ 20 kV) images were taken to investigate the surface structures of the films.

The films were investigated for the chemical composition and state of the elements using X-ray photoelectron spectroscopy (XPS; Omicron ESCA+ system; Omicron Nanotechnology GmbH equipped with a hemispherical energy analyzer at a base pressure of  $<5 \times 10^{-10}$  mbar). The survey spectra were recorded with a pass energy of 100 eV, whereas the core level spectra were recorded at a pass energy of 20 eV, leading to a full-width half maximum of the Ag 3d<sub>5/2</sub> peak of 0.77 eV. A monochromatic Al K<sub>α</sub> (1 486.7 eV) X-ray source was used, with a spot diameter of 1 mm. The spectra were measured under a take-off angle of 70° with respect to the surface plane, and under irradiation with a low energy electron beam for charge compensation (0.8 eV). The peak analysis was done with the UNIFIT,<sup>[30]</sup> using a convolution of Gaussian and Lorentzian line shapes and modeling the background with a Shirley-type function. The spectra were referenced to the position of the Au 4f<sub>7/2</sub> peak at 83.9 eV. Where indicated, removal of the superficial film layers was done by sputtering with Ar<sup>+</sup> ions with 3 keV energy for 3 min. Finally, resistivity measurements were performed on the films in the temperature range of 77–300 K in linear four probe configuration using a homemade resistivity measurement setup.

### Supporting Information

Supporting Information is available from the Wiley Online Library or from the author.

### Acknowledgements

The authors acknowledge the use of the Circular Raw MatTERS Finland Infrastructure (RAMI) at Aalto University. The authors at RUB and Paderborn University thank the SFB-TR-87 project for financial support. M.W. thanks COST-Action HERALD for funding his research stay at Aalto University.

### Conflict of Interest

The authors declare no conflict of interest.

### Data Availability Statement

Data sharing is not applicable to this article as no new data were created or analyzed in this study.

### Keywords

ALD, Copper metal film, Cu(acac)<sub>2</sub>, Direct reduction, Hydroquinone

Received: April 21, 2021

Revised: May 29, 2021

Published online: July 26, 2021

[1] H. Kim, *Surf. Coat. Technol.* **2006**, *200*, 3104.

[2] I. Cutres, *Where are my GAA-FETs? TSMC to stay with FinFET for 3nm.*

- [3] M. Leskelä, M. Ritala, *Angew. Chem. Int. Ed.* **2003**, 42, 5548.
- [4] D. J. Hagen, M. E. Pemble, M. Karppinen, *Appl. Phys. Rev.* **2019**, 6, 041309.
- [5] L. C. Kalutarage, S. B. Clendenning, C. H. Winter, *Chem. Mater.* **2014**, 26, 3731.
- [6] K. Väyrynen, K. Mizohata, J. Räisänen, D. Peeters, A. Devi, M. Ritala, M. Leskelä, *Chem. Mater.* **2017**, 29, 6502.
- [7] T. J. Knisley, T. C. Ariyasena, T. Sajavaara, M. J. Saly, C. H. Winter, *Chem. Mater.* **2011**, 23, 4417.
- [8] T. S. Tripathi, M. Karppinen, *Chem. Mater.* **2017**, 29, 1230.
- [9] K. Stoev, K. Sakurai, *Recent theoretical models in grazing incidence X-ray reflectometry*.
- [10] Y. Pauleau, A. Y. Fasasi, *Chem. Mater.* **1991**, 3, 45.
- [11] D. Briggs, *Surf. Interface Anal.* **1981**, 3, v.
- [12] H. Estrade-Szwarcckopf, *Carbon* **2004**, 42, 1713.
- [13] T. Ohta, M. Yamada, H. Kuroda, *Bull. Chem. Soc. Jpn.* **1974**, 47, 1158.
- [14] P. Martensson, J. Carlsson, *J. Electrochem. Soc.* **1998**, 145, 2926.
- [15] T. Waechtler, S.-F. Ding, L. Hofmann, R. Mothes, Q. Xie, S. Oswald, C. Detavernier, S. E. Schulz, X.-P. Qu, H. Lang, T. Gessner, *Microelectron. Eng.* **2011**, 88, 684.
- [16] A. Cabañas, X. Shan, J. J. Watkins, *Chem. Mater.* **2003**, 15, 2910.
- [17] P. A. Premkumar, N. Bahlawane, K. Kohse-Höinghaus, *Chem. Vap. Depos.* **2007**, 13, 219.
- [18] N. Bahlawane, P. A. Premkumar, F. Reilmann, K. Kohse-Höinghaus, J. Wang, F. Qi, B. Gehl, M. Bäumer, *J. Electrochem. Soc.* **2009**, 156, D452.
- [19] P. A. Premkumar, N. Bahlawane, G. Reiss, K. Kohse-Höinghaus, *Chem. Vap. Depos.* **2007**, 13, 227.
- [20] J. Huo, R. Solanki, J. McAndrew, *J. Mater. Res.* **2002**, 17, 2394.
- [21] C. Lee, H.-H. Lee, *Electrochem. Solid-State Lett.* **2005**, 8, G5.
- [22] C. Vestal, T. Devore, *Int. Symp. High Temp. Corros. Mater. Chem. Wash. DC Electrochem. Soc.* **2001**, 285.
- [23] J. Pinkas, J. C. Huffman, D. V. Baxter, M. H. Chisholm, K. G. Caulton, *Chem. Mater.* **1995**, 7, 1589.
- [24] X. Yuan, A. N. Pham, C. J. Miller, T. D. Waite, *Environ. Sci. Technol.* **2013**, 47, 8355.
- [25] S. Mandal, N. H. Kazmi, L. M. Sayre, *Arch. Biochem. Biophys.* **2005**, 435, 21.
- [26] Y. Li, M. A. Trush, *Carcinogenesis* **1993**, 14, 1303.
- [27] Y. B. Li, M. A. Trush, *Arch. Biochem. Biophys.* **1993**, 300, 346.
- [28] X. Hu, J. Schuster, S. E. Schulz, T. Gessner, *Phys. Chem. Chem. Phys.* **2015**, 17, 26892.
- [29] Z. Giedraityte, O. Lopez-Acevedo, L. A. Espinosa Leal, V. Pale, J. Sainio, T. S. Tripathi, M. Karppinen, *J. Phys. Chem. C* **2016**, 120, 26342.
- [30] R. Hesse, T. Chassé, R. Szargan, *Fresenius J. Anal. Chem.* **1999**, 365, 48.
- [31] A. U. Mane, S. A. Shivashankar, *Mater. Sci. Semicond. Process.* **2004**, 7, 343.
- [32] M. Utriainen, M. Kröger-Laukkanen, L.-S. Johansson, L. Niinistö, *Appl. Surf. Sci.* **2000**, 157, 151.
- [33] B. S. Lim, A. Rahtu, R. G. Gordon, *Nat. Mater.* **2003**, 2, 749.
- [34] Z. Li, A. Rahtu, R. G. Gordon, *J. Electrochem. Soc.* **2006**, 153, C787.
- [35] Z. Li, R. G. Gordon, D. B. Farmer, Y. Lin, J. Vlassak, *Electrochem. Solid-State Lett.* **2005**, 8, G182.
- [36] T. Waechtler, S. Oswald, N. Roth, A. Jakob, H. Lang, R. Ecke, S. E. Schulz, T. Gessner, A. Moskvina, S. Schulze, M. Hietschold, *J. Electrochem. Soc.* **2009**, 156, H453.
- [37] Z. Guo, H. Li, Q. Chen, L. Sang, L. Yang, Z. Liu, X. Wang, *Chem. Mater.* **2015**, 27, 5988.
- [38] J. P. Coyle, G. Dey, E. R. Sirianni, M. L. Kemell, G. P. A. Yap, M. Ritala, M. Leskelä, S. D. Elliott, S. T. Barry, *Chem. Mater.* **2013**, 25, 1132.
- [39] N. Boysen, B. Misimi, A. Muriqi, J.-L. Wree, T. Hasselmann, D. Rogalla, T. Haeger, D. Theirich, M. Nolan, T. Riedl, A. Devi, *Chem. Commun.* **2020**, 56, 13752.
- [40] B. H. Lee, J. K. Hwang, J. W. Nam, S. U. Lee, J. T. Kim, S.-M. Koo, A. Baunemann, R. A. Fischer, M. M. Sung, *Angew. Chem.* **2009**, 121, 4606.
- [41] B. Vidjayacoumar, D. J. H. Emslie, S. B. Clendenning, J. M. Blackwell, J. F. Britten, A. Rheingold, *Chem. Mater.* **2010**, 22, 4844.
- [42] P. Mårtensson, J.-O. Carlsson, *Chem. Vap. Depos.* **1997**, 3, 45.
- [43] T. Törndahl, J. Lu, M. Ottosson, J.-O. Carlsson, *J. Cryst. Growth* **2005**, 276, 102.
- [44] D.-Y. Moon, D.-S. Han, S.-Y. Shin, J.-W. Park, B. M. Kim, J. H. Kim, *Thin Solid Films* **2011**, 519, 3636.